Diabetes Modulates Iodothyronine Deiodinase 2 Expression in the Mouse Retina: A Role for Thyroid Hormone in the Pathogenesis of Diabetic Retinopathy

Reena Bapputty,[1] Hima Sapa,[2] Miyagi Masaru,[3] and Rose A. Gubitosi-Klug[1]

[1]Department of Pediatrics, Case Western Reserve University School of Medicine/Rainbow Babies and Children's Hospital, Cleveland, Ohio, United States
[2]Department of Nephrology and Hypertension, Case Western Reserve University School of Medicine, Cleveland, Ohio, United States
[3]Department of Pharmacology, Case Western Reserve University School of Medicine, Cleveland, Ohio, United States

PURPOSE. Clinical investigations associate hypothyroidism with an increased risk for microvascular complications, yet the mechanism by which thyroid hormone regulates the development of diabetic retinopathy is not clearly understood. We investigated the role of iodothyronine deiodinase 2 (DIO2) in the pathogenesis of diabetic retinopathy.

METHODS. Retinas from streptozotocin-induced diabetic and nondiabetic mice were evaluated by RNA sequencing, RT-PCR, and immunostaining. Media and cell lysates from mouse retinal microvascular endothelial cells and retinal astrocytes exposed to physiologic (5 mM) and high glucose (25 mM) containing media were assessed by liquid chromatography-tandem mass spectrometry to measure tetraiodothyronine (T4) and triiodothyronine (T3) concentrations and by Western blot analysis to determine the relationship of T4/T3 to oxidative stress and inflammatory mediators. Cell death was determined by Trypan Blue exclusion assay.

RESULTS. At 12 weeks of diabetes duration, retinas from diabetic mice compared with nondiabetic mice demonstrated a significant decrease in *Dio2* transcripts and *Dio2* gene and protein ($P < 0.05$) expression. When cultured in the presence of high glucose, both mouse retinal astrocytes and microvascular endothelial cells demonstrated a significant reduction of DIO2 protein compared with cells cultured in physiologic glucose. High glucose inhibited generation of T3, leading to a significantly increased T4/T3 ($P < 0.0079$). Supplementation of cells with T3, but not T4, prevented the high glucose-induced rise in endothelial nitric oxide synthase, intercellular cell adhesion molecule 1, and endothelial cell death ($P < 0.0079$).

CONCLUSIONS. Decreased intraretinal T3 owing to diabetes-induced loss of DIO2 may lead to dysfunction and death of cells in the retina, thereby contributing to the pathogenesis of early diabetic retinopathy.

Keywords: diabetic retinopathy, thyroid hormone, iodothyronine deiodinase 2, inflammation, retinal microvascular endothelial cells

Several lines of evidence demonstrate that hypothyroidism increases the risk for microvascular diseases,[1–5] yet the mechanism by which thyroid hormone impacts the pathogenesis of diabetic retinopathy has not been determined. Diabetic retinopathy, a complication of diabetes, is characterized by dysfunction of both vascular and neuronal cells.[6,7] Retinal microvascular endothelial cell degeneration resulting in acellular capillaries is one of the hallmark lesions of diabetic retinopathy.[8,9] Studies have shown that, during the early stage of diabetic retinopathy, impaired production of oxidative stress as measured by nitric oxide generation (endothelial nitric oxide synthase [eNOS]) is triggered, causing dysfunction in vasodilation.[10] Activation of inflammatory cascades induces production of intercellular adhesion molecule 1 (ICAM1) and causes further vascular

compromise.[11–14] The resultant vascular permeability and vascular occlusion lead to local areas of ischemia in the retina and, ultimately, vascular cell death and capillary degeneration.[9]

Thyroid hormone is essential for a variety of physiological processes including cell growth, differentiation, and metabolism in mammals. It improves insulin secretion and insulin signaling.[15] Compelling evidence suggests that triiodothyronine (T3), the biologically active form of thyroid hormone, is a survival factor and inhibits apoptosis in pancreatic β-cells[16] and in human luteinized granulosa cells.[17] T3 also contributes to the regulation of oxidative stress and inflammatory markers. Increased levels of TNFα, IL-6, and nitric oxide were observed in patients with overt or subclinical hypothyroidism.[18–20] Low-grade

Investigative Ophthalmology & Visual Science

inflammation causes coronary endothelial dysfunction in patients with hypothyroidism compared with euthyroid controls.[19,21] Embryologically, layering and differentiation of retinal cell types during development is dependent on T3/tetraiodothyronine (T4) levels and hypothyroid status (low T3/T4 levels) delays or alters these developmental processes.[22]

In mammals, thyroid hormone homeostasis is regulated by a feedback loop connecting the hypothalamus, pituitary, and thyroid. Thyrotropin-releasing hormone from the hypothalamus stimulates the pituitary to generate thyroid-stimulating hormone (TSH), which then binds to its receptor on the thyroid. Within the thyroid, iodinases and deiodinases regulate hormonogenesis and the storage of thyroid hormone.[23] Binding of TSH leads to release of thyroid hormone into the circulation. Ultimately, circulating thyroid hormone provides feedback to the hypothalamus to achieve homeostasis. The predominant form of circulating thyroid hormone is T4. However, the transcriptional regulation by thyroid hormone is mediated by the nuclear bound T3.[24] Various tissues express peripheral iodothyronine deiodinases, which control the local conversion of T4 to T3. T3 interacts with thyroid hormone receptors, which are members of the nuclear receptor superfamily, which can activate or repress gene transcription. Studies have shown that more than 50% of T3 in the rodent brain is locally generated by the action of deiodinases.[25] Both iodothyronine deiodinase 1 and iodothyronine deiodinase 2 (DIO2) are involved in the conversion of T4 to the biologically active hormone T3. More than 80% of plasma T3 originates from extrathyroidal pathways and clinical studies demonstrate DIO2 as the major contributor[26,27] to the cellular pool of T3 in humans.[28]

Clinically, the coexistence of hypothyroidism and diabetes is quite common.[29–33] Given that hypothyroidism in its overt or subclinical form may have deleterious effects on the complications of diabetes,[34] we investigated the expression of DIO2 in the retina using the streptozotocin-induced diabetes model in mice and studied the potential effects of thyroid hormone on the chronic inflammatory and oxidative stress cascades involved in the pathogenesis of diabetic retinopathy.

MATERIALS AND METHODS

Experimental Animals

Wild-type C57BL/6 male mice were purchased from Jackson Laboratories (Bar Harbor, ME, USA). Mice (8 weeks of age) were randomly assigned to the diabetic or nondiabetic control groups. Mice in the diabetic group were given five sequential daily, intraperitoneal injections of a freshly prepared solution of streptozotocin (60 mg/kg body weight) in citrate buffer (pH 4.5). Hyperglycemia was confirmed by checking the blood glucose at least three times during the second week after streptozotocin administration. Mice with random blood glucose of more than 250 mg/dL glucose were assigned to the diabetic group. Insulin was given as needed to achieve slow weight gain without preventing hyperglycemia and glucosuria (typically 0–0.2 U NPH insulin subcutaneously, 0–3 times per week). The animals had free access to both food and water and were maintained under a 14-hour on/10-hour off light cycle. Food consumption and body weight were measured weekly. Glycohemoglobin was measured every 2 to 3 months throughout the experiment.

All animal experiments were conducted in accordance with the ARVO Statement for the Use of Animals in Ophthalmic and Vision Research.

Cell Culture

Mouse primary retinal endothelial cells were purchased from Cell Biologics, Inc. (Chicago, IL, USA) were grown in complete mouse endothelial cell medium (M1168-Kit, Cell Biologics, Inc.) containing endothelial growth supplements; VEGF, endothelial cell growth supplement, heparin, epidermal growth factor, hydrocortisone, L-glutamine, antibiotic–actinomycotic solution, and 5% fetal bovine serum (FBS). The cells were received at passage 3 and the experiments conducted from passage 5 to passage 11. Primary retinal microvascular endothelial cells are characterized by immunofluorescence staining with antibodies of VE-cadherin (CD144, VE-cadherin Antibody, C-19, sc6458, Santa Cruz Biotechnology, Dallas, TX, USA), AF1002 (R&D Systems, Minneapolis, MN, USA) or CD31/PECAM-1 (Catalog No. 553370, Becton Dickinson, Franklin Lakes, NJ, USA) by Cell Biologics Inc. These cells are devoid of bacteria, yeast, fungi, and mycoplasma contamination as tested by our Visual Science Research Core facility using spectrophotometric method and confirmed again by DNA staining using Hoechst fluorochrome and visualizing under a fluorescence microscope.

The mouse retinal astrocytes (mAST) were kindly provided by N. Sheibani (University of Wisconsin, Madison, WI, USA) and were originally isolated from Immortomice[35] were grown in DMEM containing 10% FBS. Cells were seeded and grown in a 60-mm dish for all experiments except for immunolabeling experiments. Retinal astrocytes and microvascular endothelial cells (mRECs) were grown in control medium (containing 5.5 mM glucose) or high-glucose medium (containing 25 mM glucose) and were cultured at 37°C in 5% CO_2. Media was changed every other day for 5 days. Thyroxine (Sigma, St. Louis, MO, USA) and T3 (Sigma) were dissolved in 1 N NaOH at 1 mg/mL concentration and further dilution was in 0.5% FBS-containing media for mRECs and in 1% FBS containing media for mAST. For immunofluorescence staining, Western blotting, and mass spectrometry analysis, media was exchanged to media containing 0.5% or 1% FBS on day 4, when cells were at approximately 85% confluency, T3 or T4 was added and incubated overnight.

RNA Sequencing

Total RNA Preparation and RNA Sequencing Library Preparation. Retinas were collected from control and 12-week diabetic mice and flash frozen on dry ice. Total RNA was extracted with the RNeasy Plus Mini Kit (Qiagen, Germantown, MD, USA). RNA quality was confirmed using the 2100 Bioanalyzer (Agilent Technologies; Santa Clara, CA). All RNA samples had an RNA integrity number of greater than 9.0. Samples were prepared for sequencing following Illumina TruSeq-style library preparation protocol. Enrichment of mRNA was done following rRNA depletion method (NEBNext rRNA Depletion Kit (Human/Mouse/Rat), E6310X) and RNA libraries were prepared using the NEBNext Ultra II Directional RNA Library Prep Kit for Illumina (96RXNS) (New England Biolabs, Ipswich, MA, USA; E7760L). Library quality was assessed using the 2100 Bioanalyzer. Sequencing was performed using a single read, 75-bp

protocol on the Illumina HiSeq 2500 (Illumina, San Diego, CA, USA).

Sequencing reads generated from the Illumina platform were assessed for quality and trimmed for adapter sequences using Trim Galore v0.4.2 (Babraham Bioinformatics, Cambridge, UK), a wrapper script for FastQC and cutadapt. Reads that passed quality control were then aligned to the mouse reference genome (mm10) using the STAR aligner v2.5.1. The aligned reads were analyzed for differential expression using Cufflinks v2.2.1, an RNA sequencing analysis package which reports the fragments per kilobase of exon per million fragments mapped for each gene. Differential analysis report was generated using the cuffdiff command performed in a pairwise manner for each group. Differential genes were identified using a significance cutoff of q-value of less than 0.05. The list of differentially expressed genes in the retina between nondiabetic and diabetic mice has been uploaded to the Gene Expression Omnibus. The genes were then subjected to gene set enrichment analysis (Gene Pattern, Broad Institute, Cambridge, MA, USA) to determine any relevant processes that may be differentially over-represented for the conditions tested.[36,37] All of these processes were performed at the Institute for Computational Biology, Case Western Reserve University.

Real-time PCR

Total RNA was isolated from 12 week-diabetic and control mice retina using RNeasy Plus Mini Kit (Qiagen, Germantown, MD, USA). First strand cDNA was synthesized using Superscript III first-strand synthesis super mix for quantitative RT-PCR (Invitrogen, Carlsbad, CA, USA). Real-Time PCR primers were designed using primer quest tools (IDT, Coralville, IA, USA) and synthesized by IDT. Primer sequences for *Dio2* forward, CGATTGATGTGGCTCCCTAAA and reverse TCTGACTTTCTGCTTCGCTATC were used for the amplification. Beta-actin forward (5′-GAGGTATCCTGACCCTGAAGTA-3′) and reverse (5′-CACACGCAGCTCATTGTAGA-3′) was used as the housekeeping gene. Real-time PCR was performed following the SYBR green quantitative PCR super mix for iCycler (Invitrogen, Carlsbad, CA, USA). PCR primer sequences were designed with primer quest tools (IDT).

Immunofluorescence Staining of Retinal Sections and Retinal Cells

DIO2 in formalin-fixed and paraffin-embedded retinal sections of nondiabetic control and 28-week diabetic mice was detected and quantified by immunofluorescence. Briefly, tissue sections were deparaffinized using three changes of xylene and rehydrated using different concentrations of alcohol washes. Antigen retrieval was done using Tris (10 mM EDTA [1 mM] TWEEN-20 [0.05%] pH 9 by microwaving for a total of 15 minutes (3 times, 5 minutes each). The tissue sections were blocked for 1 hour in 1% BSA in PBS and were stained with primary antibody (ab-77779 1:200) overnight at 4°C. The secondary antibodies were goat anti-rabbit Alexa fluor 568 (Orange) was used at 1:500 dilution. Sections were then washed using PBS and incubated with DAPI (Molecular Probes, Invitrogen detection technologies, Carlsbad, CA, USA) for 10 minutes to label the nucleus. Omitting the primary antibodies in the incubation reaction gave no signal.

For immunofluorescence labeling of DIO2 and eNOS in cells, mREC or mAST were plated and grown on poly-L-lysine–coated glass coverslips for 5 days either in normal or high glucose media. On day 4, media was exchanged to include media containing 0.5% FBS (for mREC) or 1.0% FBS (for mAST) and T3 or T4 was added to the cultures and incubated overnight. On day 5, media was removed, cells were washed with PBS, and cells were fixed with 4% paraformaldehyde for 20 minutes. Blocking was in 3% BSA in PBST (TWEEN-20 0.05%) for 30 minutes. Primary antibody, rabbit polyclonal to DIO2 (ab-77779, 1:1000, incubated overnight); or rabbit monoclonal to eNOS (ab-199956, 1:250, at RT for 2 hours, Abcam, Cambridge, MA, USA) was applied followed by secondary antibody Alexa Fluor 568 (1:500, Invitrogen A-1101, Grand Island, New York, USA) for 1 hour.

The immuno-labeled retinal sections and retinal cells were imaged on an Olympus FV1200 confocal laser scanning microscope (Olympus, Center Valley, PA, USA) with a 40× UPlanFL N objective (NA;1.40) with oil. DAPI was used for staining the cell nuclei and was detected by exciting the sample with a 405-nm diode laser and the emission signal was collected at 425 to 460 nm. Alexa Fluor 568 was detected by exciting the sample with a 559 nm diode laser and the emission signal was collected at 575 to 620 nm. Sequential scanning mode was used to avoid crosstalk between channels. Images were processed with FluoView software. DIO2 level was expressed as relative mean fluorescence intensity.

Mass Spectrometry

Total T3 and T4 concentrations in mREC cell lysate and media were measured by a liquid chromatography-multiple reaction monitoring (LC-MRM) based method. Cell culture media was collected and stored at −80°C until processing for T3 or T4 extraction. For cell lysate, cells were washed twice with PBS and lysed using 200 μL ice-cold acetonitrile (75%) in water containing 1% NH_3OH. Then, internal standards $^{13}C_6$-T3 and $^{13}C_6$-T4 (Toronto Research Chemicals, Toronto, Ontario, Canada) were added (20 pmol each) and the whole cell extract was collected, vortexed for 30 seconds, and centrifuged at $16,000 \times g$ for 10 minutes. The supernatant was collected and dried using a speed vacuum concentrator. The sample was then reconstituted in DMSO: 0.1% formic acid in water (1:1) and analyzed by LC-MRM using an Agilent 6460 Triple Quad LC/MS system (San Jose, CA, USA).

T3 and T4 from mREC media (DMEM without phenol red) was extracted along with internal standards following the method of Rathmann et al.[38] To 400 μL medium, ice-cold internal standards $^{13}C_6$-T3 and $^{13}C_6$-T4 (20 pmol each) were added, and the medium was acidified by adding 5 μL 30% HCl, vortexed for 20 seconds and incubated at 37°C for 30 minutes in the dark. T3 and T4 were then extracted by adding 1 mL of freshly prepared propanol/trimethyl butyl ether (30:70 v/v). The upper phase was collected. The propanol/trimethyl butyl ether extraction was repeated one more time. The combined upper phase was evaporated to dryness by a stream of nitrogen gas and reconstituted in DMSO: 0.1% formic acid in water (1:1) by vertex mixing for 20 seconds. The samples were centrifuged at 14,000 rpm for 10 minutes and analyzed by LC-MRM-MS.

Standard curves were made with T4 (0.024–6.25 nM for cell lysate and 0.024–50.00 nM for media, Sigma) and T3 (0.024–6.25 nM, for cell lysate and 0.024–50 nM; Sigma) for

media. Each concentration of T3 and T4 standards were processed the same way as samples. Internal standards $^{13}C_6$-T3 and $^{13}C_6$-T4 (20 pmol each) were added to the 200 µL of standard, vortex-mixed, centrifuged, vacuum-dried, reconstituted in DMSO:0.1% formic acid in water (1:1). Analytes were separated using reverse phase C18 column (Phenomenex 2.6 µm 100 Å, 100.0 × 2.1 mm) with a linear gradient of acetonitrile from 25% to 60% in water in the presence of 0.1% formic acid over a period of 8 minutes at a flow rate of 0.2 mL/min. Nitrogen gas was used as the nebulizer and collision gas. Injection volume was 10 µL. Analytes were monitored by MRM in positive ion mode with collision energy at 25 V for all the compounds. Agilent Mass Hunter software 10.0 was used for all data acquisition and quantification. The MRM transitions used were m/z 651.8 → 605.8 for T3, 777.7 → 731.7 for T4, 657.8 → 611.8 for $^{13}C_6$-T3, and 783.7 → 737.7 for $^3C_6$-T4. Standard curves were linear ($r^2 = 0.997$ for T3, $r^2 = 0.998$ for T4) over the concentration range of 0.024 to 6.25 nM for both T3 and T4.

Total T3 and T4 concentrations in the media and in cell lysate were calculated by normalizing the value to total cell number. For that, just before cell harvest, phase contrast microscopy images of cells in the dishes were taken with a 10×/0.30-NA objective on a Leica microscope (Leica Microsystems, Buffalo, NY, USA). Images of cells at nine regions in dishes (center of the plate, two points, 1 and 2 cm apart from the center to each right, left, top, and bottom)

were taken using a program set up on Metamorph Imaging Software (Molecular Devices, San Jose, CA, USA). The total number of cells were quantified by extrapolating areas from nine regions to the total area of the dish. Thyroid hormones T3 and T4 in the media and in cell lysate were expressed as femtomoles per million cells.

Western Blotting

Cells were harvested using cell lysis buffer, sonicated, centrifuged and the supernatants were used for immunoblotting. Proteins (20–30 µg) were separated on a sodium dodecyl-sulfate polyacrylamide gel electrophoresis and electroblotted onto nitrocellulose membranes. Membranes were blocked using blocking buffer from Li-COR Biosciences. Primary antibodies used were rabbit polyclonal to ICAM1 (10020-1-AP, 1:1000, Proteintech, Rosemont, IL, USA), rabbit monoclonal to eNOS (ab199956, 1:1000, Abcam), goat polyclonal to tubulin (ab21057 1:1000, Abcam) were applied for overnight at 4°C followed by secondary antibodies IRDye 800CW, donkey anti-rabbit (926-32213, 1:5000), IRDye 680RD, donkey anti-goat (926-68074, 1:5000) from Li-COR Biosciences (Lincoln, NE, USA) for 1 hour at room temperature. The immunoblots were visualized using LiCOR Odyssey Imaging System and the band intensity was measured using Image studio software (Li-COR Biosciences). Data represent the results from four to five experiments.
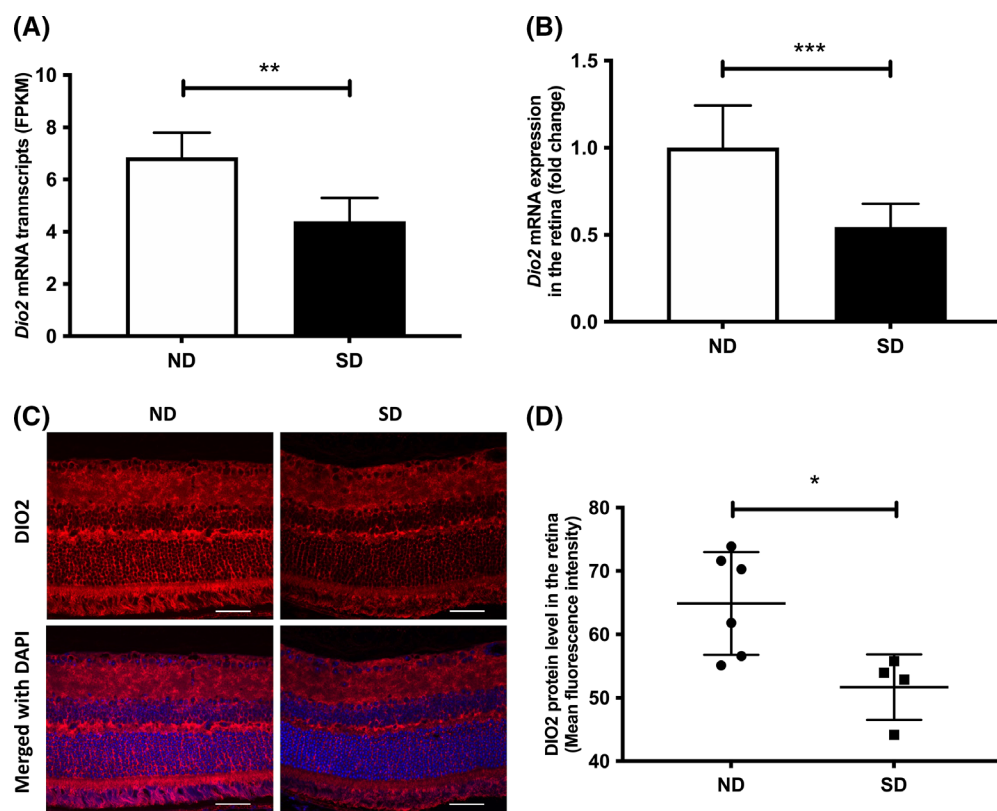
Figure 1. Diabetes regulates *Dio2* in the retina. Using the RNA sequencing (**A**) and real-time quantitative PCR (**B**) techniques, the retinas from the diabetic mice (SD, black bar, 12 weeks of diabetes duration, $n = 6$) demonstrated decreased *Dio2* mRNA transcripts compared with the retinas from nondiabetic control mice (*ND, white bar, $n = 6$*). $P < 0.004$ (RNA seq) and $P < 0.001$ (real time PCR). (**C**) Mouse retinal sections were analyzed for DIO2 expression by immunofluorescence staining revealed presence of DIO2 throughout the retinal layers. All images shown correspond to the maximum intensity projection of a z-stack. (**D**) Decreased DIO2 expression is detected in the retinas of diabetes mice (*squares; $n = 4$*) at 28 weeks of diabetes duration compared with retinas from nondiabetic mice (*circles,; $n = 6$*) as measured by mean fluorescence intensity ($P < 0.05$). Scale bar, 50 µm.

(A)

(B)
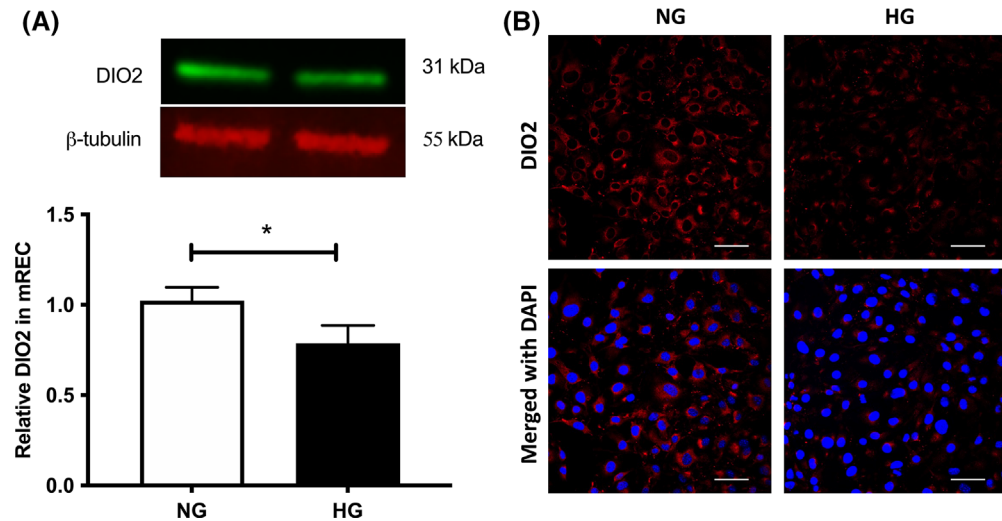
FIGURE 2. High glucose inhibits DIO2 protein expression in retinal endothelial cells. Primary mouse retinal endothelial cells were grown in physiologic (5.5 mM, NG) or high (25 mM, HG) glucose for 5 days. On day 4, media was exchanged with 0.5% FBS containing media and treatment with T3 (1 nM) or T4 (1 nM) was for overnight. Growing cells in high glucose (*black bar*) resulted in decreased DIO2 protein expression measured by (**A**) Western blot analysis ($P < 0.02$) compared with cells grown in physiologic glucose (*white bar*). (**B**) immunofluorescence staining of mREC for DIO2. Scale bar, 50 µm. Data are representative of four independent experiments.

Supplementation of Cultured Cells With Thyroid Hormone and Cell Death Assay

Mouse primary retinal endothelial cells were cultured for 5 days in either physiologic or high glucose media. Media was changed every other day. T3 (1 nM) or T4 (1 nM) were added to the medium for the entire 5 days in culture. Cell viability was measured by Trypan Blue exclusion assay. Briefly, an aliquot of cell suspension was diluted 1:1 (vol/vol) with 0.4% Trypan Blue, and the cells were counted with a hemocytometer. Cell death was defined as the percentage of blue-stained cells or dead cells versus the total number of cells.

Statistical Analysis

Results are expressed as means ± SD. The data were analyzed by the nonparametric Kruskal-Wallis test followed by the Mann–Whitney *U* test. Differences were considered statistically significant when the *P* was less than 0.05.

RESULTS

Glycemic Control in Mice

Diabetic mice at 12-week and 28-week diabetes duration had greater concentrations of fasting blood glucose

(A)

(B)
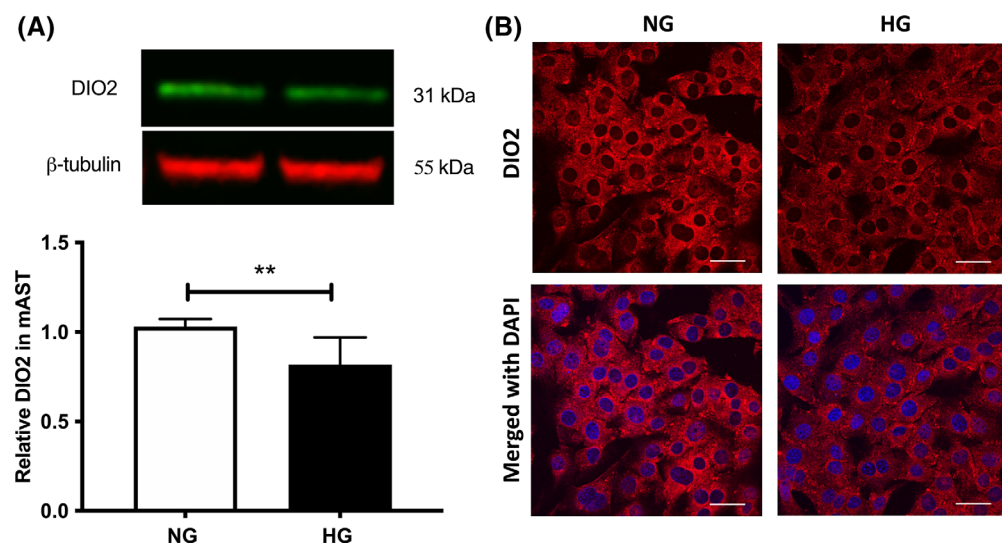
FIGURE 3. High glucose suppresses DIO2 protein expression in astrocytes. Astrocytes have been implicated in chronic inflammatory processes in diabetic retinopathy. (**A**) Western blot analysis of DIO2 protein in mAST grown in high glucose (25 mM [HG]; *black bar*) for 5 days demonstrated a decreased DIO2 protein expression compared with cells grown in physiologic glucose (5.5 mM [NG]; *white bar*). Treatment with T3 (1 nM) or T4 (1 nM) was in 1.0% FBS-containing media for overnight. (**B**) immunofluorescence staining of mREC for DIO2. Scale bar, 50 µm. Data are representative of the results from five independent experiments ($P < 0.002$).
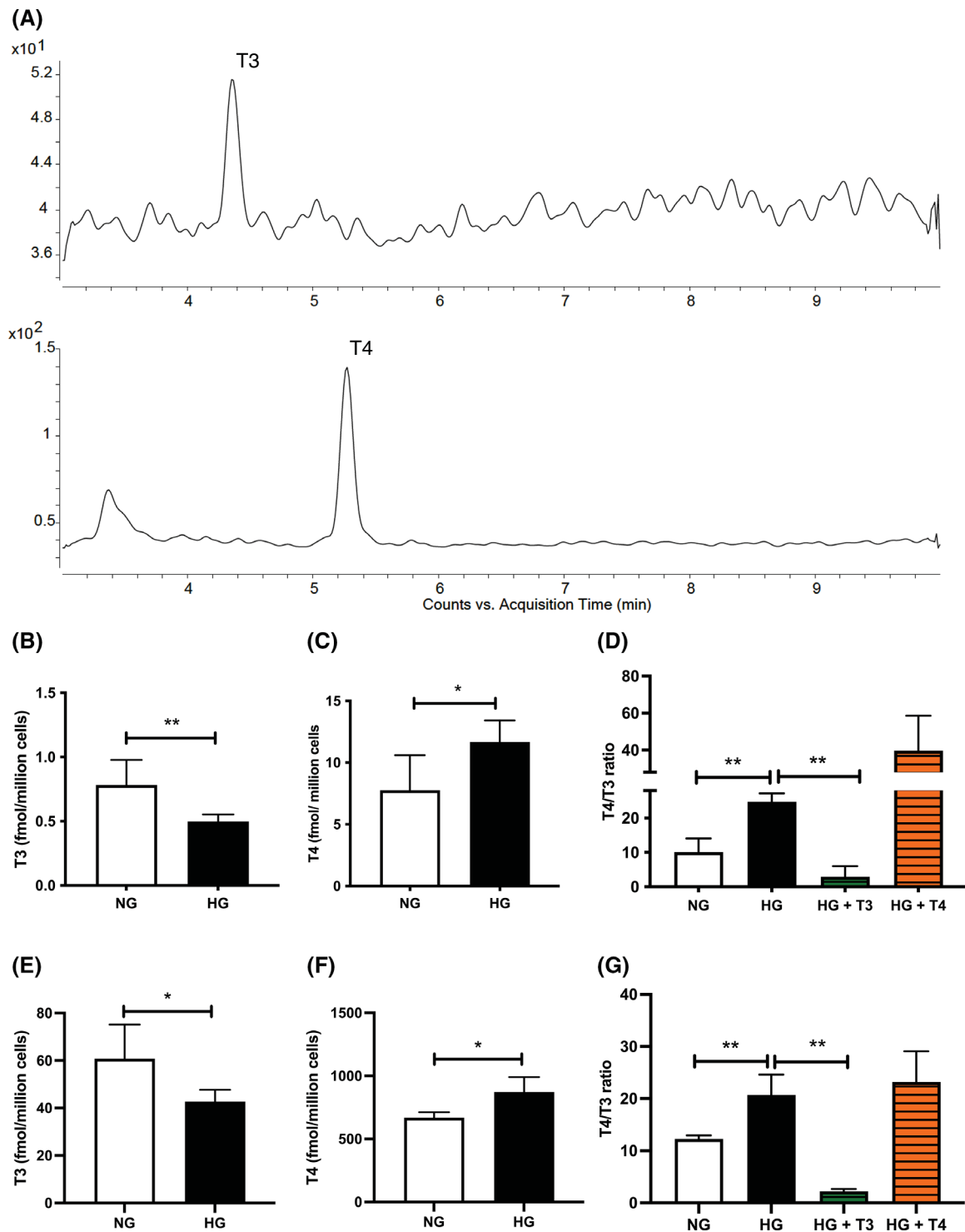
FIGURE 4. High glucose decreases intracellular T3 concentration and increases intracellular T4/T3 in mREC. (**A**) Representative image of a MRM chromatograms of T3 (0.029 nM) and thyroxine (T4, 0.350 nM) in mouse primary retinal endothelial cell lysate. Cells were grown in physiologic (5.5 mM, NG) or high glucose (25 mM [HG]) conditions for 5 days. On day 4, media was exchanged to 0.5% FBS containing media without phenol red and treatment with T3 (1 nM) or T4 (1 nM) was for overnight. High glucose inhibited (**B**) intracellular T3 synthesis, which resulted in decreased cellular T3 concentration ($P < 0.0087$), (**C**) increased T4 level ($P < 0.0317$), and (**D**) increased T4/T3 ratio ($P < 0.0079$). Supplementing T3 improved high glucose-induced rise in intracellular T4/T3 ratio, which was not achieved with T4 treatment. Analysis of cell culture media reflected the intracellular thyroid hormone levels. High glucose conditions resulted in decreased T3 (**E**) $P < 0.0159$ and increased T4 (**F**) $P < 0.0317$ levels in media compared with media of cells grown in normal glucose. Addition of T3 showed improved T4/T3 ratio (**G**) $P < 0.0079$ in cells grown under high conditions. Details of mass spec conditions are given in the method section. Data are representative of results from five independent experiments.
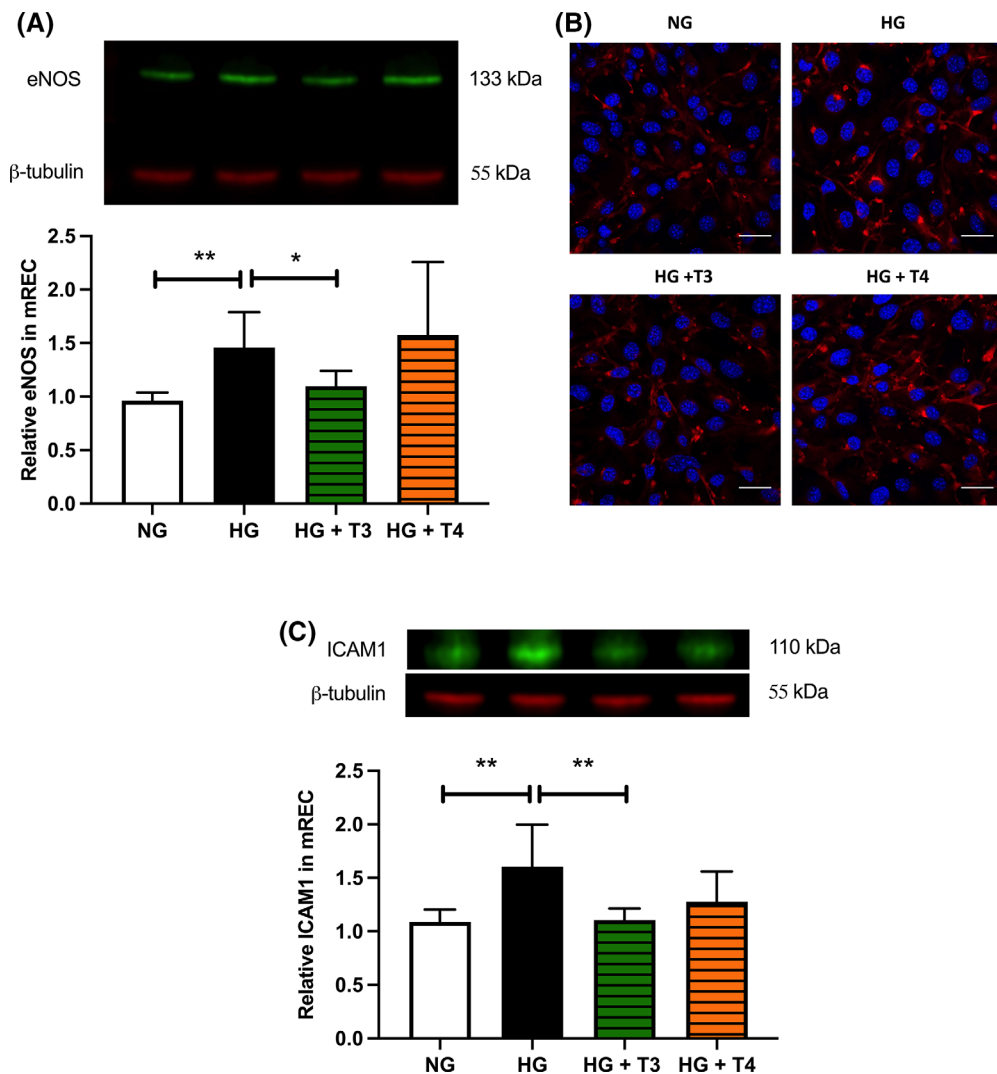
FIGURE 5. T3 inhibits high glucose-induced oxidative stress and inflammatory markers in mREC. Cells were grown in physiologic (5.5 mM) or high (25 mM) glucose conditions for five days. On day 4, media was exchanged with 0.5%FBS media and T3 (1 nM) or T4 (1 nM) was added and incubated overnight. eNOS expression was analyzed by (**A**) Western blot analysis and (**B**) immunofluorescence staining. High glucose induced eNOS expression in cells grown in high glucose ($P < 0.0079$). Treatment with T3 but not T4 attenuated high glucose-induced eNOS levels in mREC ($P < 0.03$). Confocal microscopy of mREC stained for eNOS (*red*) expression was observed mainly in the Golgi. The nuclei were stained with DAPI (*blue*). (**C**) Increased ICAM1 expression was observed in cells grown in high glucose ($P < 0.002$) compared with cells grown in physiologic glucose. Similar to eNOS, treatment with T3 but not T4 prevented high glucose induced ICAM1 level in mREC ($P < 0.004$). Scale bar, 50 µm. NG, physiologic glucose; HG, high glucose. Data are representative of the results from four or five independent experiments.

(577 ± 17 mg/dL vs. 528 ± 29 mg/dL for 12-week diabetic mice vs. 28-week diabetic mice) and glycohemoglobin ($9.34 \pm 0.95\%$ vs. $10.88 \pm 0.84\%$ for 12-week diabetic mice vs. 28-week diabetic mice) compared with their age-matched, nondiabetic controls (177 ± 18 mg/dL vs. 148 ± 25 mg/dL for nondiabetic control of 12-week diabetic mice vs. 28-week diabetic mice) and glycohemoglobin ($1.28 \pm 0.82\%$ vs. $3.74 \pm 0.09\%$ for nondiabetic control of 12-week diabetic mice vs. 28-week diabetic mice).

Dio2 in the Mouse Retina During Diabetes

RNA sequencing of retinal samples from 12-week streptozotocin-induced diabetic mice demonstrated a significant decrease in *Dio2* mRNA transcript, one of the top 100 differentially expressed gene identified (Supplementary Fig. S1), compared with nondiabetic control mice (Fig. 1A). The gene expression pattern was confirmed by real-time quantitative PCR and the result showed nearly a 50% decrease in *Dio2* expression in the retinas from streptozotocin-induced diabetic mice compared with nondiabetic control mice (Fig. 1B). To understand where in the retina local thyroid hormone production occurs, we examined retinal cross-sections by the immunofluorescence method. Evaluation of confocal images of retinal sections revealed that DIO2 is diffusely expressed in multiple layers of the retina, as reported previously[39] (Fig. 1C). Measuring the fluorescence intensity of DIO2 in retinal layers indicated that the protein expression is significantly decreased in the retina from streptozotocin-induced

diabetic mice compared with nondiabetic control mice (Fig. 1D).

Effect of High Glucose on DIO2 Protein Expression in Retinal Cells

To mimic diabetic-like conditions, cells were grown in high glucose (25 mM glucose) and compared its effect on DIO2 protein expression with cells grown in physiologic glucose (5 mM glucose) using Western blotting. Growing mREC under high glucose conditions for 5 days inhibited DIO2 protein expression by more than 20% compared with cells grown in physiologic glucose (Fig. 2A). Immunofluorescence staining of mREC for DIO2 correlated with the Western blot results (Fig. 2B). The decreased staining for DIO2 was observed around the nuclei, in agreement with the known localization of DIO2 in the endoplasmic reticulum.

DIO2 expression in mAST was also influenced by high glucose concentration in the media. A significantly decreased DIO2 level was observed in cells grown in high glucose compared with normal glucose (Figs. 3A and 3B) ($P < 0.002$).

High Glucose Impaired Intracellular Thyroid Hormone Concentration in mREC

Thyroid hormone levels in cell lysates and in culture media were measured by LC-MRM-MS methods. Representative MRM chromatograms of T3 and T4 in cell lysate are shown in Figure 4A. Mouse retinal endothelial cells were grown in physiologic or high glucose conditions for 5 days. A significantly decreased T3 level was observed in cells grown under high glucose conditions compared with physiologic glucose (Fig. 4B). Because T4 to T3 conversion is suppressed within the cells under high glucose conditions, increased intracellular T4 is detected (Fig. 4C), leading to an increased T4/T3 ratio in mREC (Fig. 4D). Treatment with 1 nM T3, but not 1 nM T4, improved the intracellular T3 concentration in mREC (Fig. 4D). Overall, the T4/T3 ratio was similarly elevated in cells grown in high glucose as well as cells treated with T4 (Fig. 4D). To confirm that the decrease in T3 did not reflect release of T3 into the extracellular media, the media from endothelial cells under high glucose conditions were analyzed for thyroid hormone levels. Thyroid hormone levels in the media corroborated the intracellular T3 and T4 concentrations, showing decreased T3 (Fig. 4E) and increased T4 (Fig. 4F) levels in the media of cells grown under high glucose conditions compared with physiologic conditions. T4/T3 ratio was similarly elevated in media of cells grown under high glucose as well as cells treated with T4 (Fig. 4G) ($P < 0.0079$).

T3 Inhibits High Glucose-induced Oxidative Stress and Inflammatory Markers in mREC

Previous studies have demonstrated that the high glucose condition increases nitric oxide synthase expression in endothelial cells.[40–42] Here we wanted to see the effect of supplementation of thyroid hormones on eNOS expression in mREC. High glucose containing media resulted in elevated levels of eNOS (Figs. 5A and 5B) in mREC compared with cells grown in physiologic glucose. Addition of T3 to the culture medium reduced the high glucose-induced increase in eNOS production by the endothelial cells (Figs. 5A
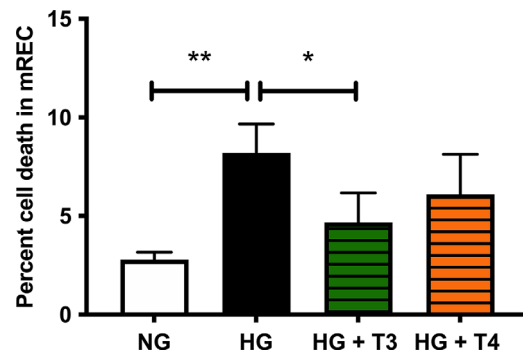
FIGURE 6. T3 protects mREC from high glucose-mediated cell death. Endothelial cells were grown in physiologic glucose (5.5 mM [NG]) or high (25 mM [HG]) glucose media for 5 days. Media was changed every other day. Fresh hormones were added every day to maintain the desired experimental condition. Increased cell death was observed, when mouse retinal endothelial cells were grown in a HG condition compared with cells grown in physiologic glucose ($P < 0.0079$). Supplementation of T3 but not T4 protected high glucose induced cell death in mREC ($P < 0.03$). Data are representative of the results from five independent experiments.

and 5B). However, treatment with T4 was not effective in bringing down high-glucose-induced eNOS in mREC.

Increased ICAM1 expression is known to induce adhesion of circulating leukocytes to the vascular endothelium. ICAM1 blockade using monoclonal antibodies prevented retinal leukostasis and vascular leakage in rat models of streptozotocin-induced diabetes.[43] Increased expression of ICAM1 was observed in cells grown in high glucose compared with normal glucose in mREC (Fig. 5C), as previously demonstrated.[44] Treatment with T3 was more effective than T4 in inhibiting the high glucose-induced expression of ICAM1 in mREC.

T3 Protects mREC From High Glucose-mediated Cell Death

Analysis of degenerate capillaries in the retina resulting from endothelial cell death is a measure for the assessment of diabetic retinopathy in a research setting. An increased amount of vascular as well as neuronal cell loss was observed in the retina during diabetes. Previous studies have demonstrated high glucose alone induces cell death in in vitro experiments.[45] Here, we tested the effect of T3 and T4 on high glucose–induced cell death in mREC. Growing cells in high glucose for 5 days induced cell death (Fig. 6) and supplementation of T3, but not T4, protected mREC from high glucose–mediated cell death (Fig. 6).

DISCUSSION

DIO2 is an intracellular regulatory enzyme of thyroid hormone metabolism essential for maintaining the local active thyroid hormone levels in cells and tissues.[24] Our current study demonstrated that in vivo or in vitro exposure of retinal cells to elevated glucose concentrations resulted in a significant decrease in DIO2 expression compared with physiologic glucose concentrations. The decrease in DIO2 expression resulted in decreased enzymatic conversion of T4 to T3, dampening the intracellular active thyroid hormone levels and resulting in an increased T4/T3 in
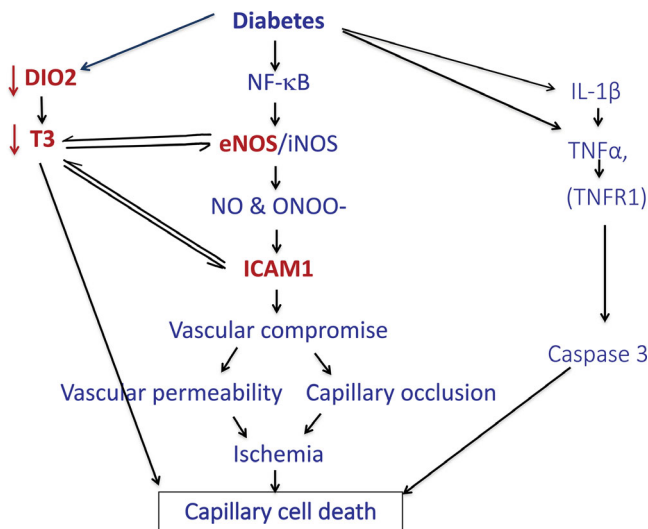
FIGURE 7. Effect of thyroid hormone on the pathophysiology of diabetic retinopathy. This schematic depicts the potential role of thyroid hormone in the regulation of inflammatory cascades and capillary degeneration in the retina during diabetes.

retinal endothelial cells. Decreased T3 levels exacerbated expression of oxidative stress and inflammatory markers in mREC, which are part of the chronic inflammatory state leading to endothelial cell death (Fig. 7). Thus, early detection of hypothyroidism and supplementation with thyroid hormone, specifically to achieve normalization of T3 concentrations, may be beneficial in the prevention of diabetic retinopathy.

Diabetes mellitus and thyroid disease are two closely associated endocrine disorders. Epidemiological studies conducted in different ethnic groups reported that the prevalence of thyroid dysfunction is higher in subjects with diabetes compared with those without diabetes and it is estimated to affect 6% to 20%[46] of individuals living with type 2 diabetes and the prevalence is much higher in the type 1 diabetes population. Patients with type 1 diabetes develop thyroid dysfunction at an early age compared with the general population and one out of four children with type 1 diabetes are prone to developing autoimmune hypothyroidism.[47,48]

Similar to our results, other vascular beds are sensitive to the extrathyroidal synthesis of thyroid hormone. Studies using rat aorta media and human coronary artery vascular smooth muscle cells and endothelial cells demonstrate that local intracellular production of T3 by DIO2 plays an important role in regulating vascular homeostasis.[49] In addition, clinical studies have demonstrated an increased level of oxidative stress and inflammatory markers (e.g., nitric oxide, C-reactive protein, IL-6, and TNF-α) in the plasma of subjects with subclinical and overt hypothyroid conditions[18,21] and has been associated with microvascular dysfunction.[19]

One of the most common strategies for the treatment of hypothyroidism is ʟ-levothyroxine administration. However, some hypothyroid patients on levothyroxine treatment remain symptomatic, even after normalization of serum TSH levels.[50] These patients present with higher serum total and free T4 and approximately 10% lower serum total and free T3 levels compared with controls,[51] which resulted in

an increased serum T4/T3. The normalization of cellular T3 may be important to follow in addition to normalization of TSH with levothyroxine treatment.

Thyroid hormone action depends on the bioavailability of active thyroid hormone, which again depends on the expression and activity of local iodothyronine deiodinases. *Dio2* (Thr92Ala) polymorphism observed in subjects with insulin resistance,[51] thus, there may also be genetic predisposition to the effects of thyroid hormones on the development of diabetes-related organ pathology.

Our study is limited by the use of the mouse model and mouse retinal cell lines, which may or may not translate to similar findings in humans. Yet, these animal studies do highlight a modifiable, adjuvant treatment to potentially alter the course of diabetic retinopathy. Combination therapy for hypothyroidism with T4 and T3 is attaining more attention these days. However, further study is needed to better understand treatment approaches and therapeutic targets for hypothyroidism and the likelihood of beneficial effects on diabetic retinopathy and other complications of diabetes.

References

1. Yang JK, Liu W, Shi J, Li YB. An association between subclinical hypothyroidism and sight-threatening diabetic retinopathy in type 2 diabetic patients. *Diabetes Care*. 2010;33:1018–1020.

2. Lin Y, Sun Z. Thyroid hormone ameliorates diabetic nephropathy in a mouse model of type II diabetes. *J Endocrinol*. 2011;209:185–191.

3. Kim BY, Kim CH, Jung CH, Mok JO, Suh KI, Kang SK. Association between subclinical hypothyroidism and severe diabetic retinopathy in Korean patients with type 2 diabetes. *Endocr J*. 2011;58:1065–1070.

4. Schultheiss UT, Daya N, Grams ME, et al. Thyroid function, reduced kidney function and incident chronic kidney disease in a community-based population: the Atherosclerosis Risk in Communities study. *Nephrol Dial Transplant*. 2017;32:1874–1881.

5. Vemula SL, Aramadaka S, Mannam R, et al. The impact of hypothyroidism on diabetes mellitus and its complications: a comprehensive review. *Cureus*. 2023;15:e40447.

6. Bapputty R, Talahalli R, Zarini S, Samuels I, Murphy R, Gubitosi-Klug R. Montelukast prevents early diabetic retinopathy in mice. *Diabetes*. 2019;68:2004–2015.

7. Gubitosi-Klug RA, Talahalli R, Du Y, Nadler JL, Kern TS. 5-Lipoxygenase, but not 12/15-lipoxygenase, contributes to degeneration of retinal capillaries in a mouse model of diabetic retinopathy. *Diabetes*. 2008;57:1387–1393.

8. Engerman RL. Pathogenesis of diabetic retinopathy. *Diabetes*. 1989;38:1203–1206.

9. Tang J, Kern TS. Inflammation in diabetic retinopathy. *Prog Retin Eye Res*. 2011;30:343–358.

10. Joussen AM, Poulaki V, Qin W, et al. Retinal vascular endothelial growth factor induces intercellular adhesion molecule-1 and endothelial nitric oxide synthase expression and initiates early diabetic retinal leukocyte adhesion in vivo. *Am J Pathol*. 2002;160:501–509.

11. Talahalli R, Zarini S, Tang J, et al. Leukocytes regulate retinal capillary degeneration in the diabetic mouse via generation of leukotrienes. *J Leukoc Biol*. 2013;93:135–143.

12. Kern TS, Du Y, Tang J, et al. Regulation of adrenergic, serotonin, and dopamine receptors to inhibit diabetic retinopathy: monotherapies versus combination therapies. *Mol Pharmacol*. 2021;100:470–479.

13. Lessieur EM, Liu H, Saadane A, Du Y, Kiser J, Kern TS. ICAM-1 on the luminal surface of endothelial cells is induced to a greater extent in mouse retina than in other tissues in diabetes. *Diabetologia*. 2022;65:1734–1744.

14. Abcouwer SF, Shanmugam S, Muthusamy A, et al. Inflammatory resolution and vascular barrier restoration after retinal ischemia reperfusion injury. *J Neuroinflammation*. 2021;18:186.

15. Lin Y, Sun Z. Thyroid hormone potentiates insulin signaling and attenuates hyperglycemia and insulin resistance in a mouse model of type 2 diabetes. *Br J Pharmacol*. 2011;162:597–610.

16. Verga Falzacappa C, Panacchia L, Bucci B, et al. 3,5,3′-triiodothyronine (T3) is a survival factor for pancreatic beta-cells undergoing apoptosis. *J Cell Physiol*. 2006;206:309–321.

17. Di Paolo V, Mangialardo C, Zacà C, et al. Thyroid hormones T3 and T4 regulate human luteinized granulosa cells, counteracting apoptosis and promoting cell survival. *J Endocrinol Invest*. 2020;43:821–831.

18. Wajner SM, Goemann IM, Bueno AL, Larsen PR, Maia AL. IL-6 promotes nonthyroidal illness syndrome by blocking thyroxine activation while promoting thyroid hormone inactivation in human cells. *J Clin Invest*. 2011;121:1834–1845.

19. Taddei S, Caraccio N, Virdis A, et al. Low-grade systemic inflammation causes endothelial dysfunction in patients with Hashimoto's thyroiditis. *J Clin Endocrinol Metab*. 2006;91:5076–5082.

20. Marchiori RC, Pereira LAF, Naujorks AA, et al. Improvement of blood inflammatory marker levels in patients with hypothyroidism under levothyroxine treatment. *BMC Endocr Disord*. 2015;15:32.

21. Sara JD, Zhang M, Gharib H, Lerman LO, Lerman A. Hypothyroidism is associated with coronary endothelial dysfunction in women. *J Am Heart Assoc*. 2015;4:e002225.

22. Sevilla-Romero E, Munoz A, Pinazo-Duran MD. Low thyroid hormone levels impair the perinatal development of the rat retina. *Ophthalmic Res*. 2002;34:181–191.

23. Suzuki K, Mori A, Lavaroni S, et al. Thyroglobulin regulates follicular function and heterogeneity by suppressing thyroid-specific gene expression. *Biochimie*. 1999;81:329–340.

24. Gereben B, Zavacki AM, Ribich S, et al. Cellular and molecular basis of deiodinase-regulated thyroid hormone signaling. *Endocr Rev*. 2008;29:898–938.

25. Kunisue T, Fisher JW, Kannan K. Determination of six thyroid hormones in the brain and thyroid gland using isotope-dilution liquid chromatography/tandem mass spectrometry. *Anal Chem*. 2011;83:417–424.

26. Schimmel M, Utiger RD. Thyroidal and peripheral production of thyroid hormones. Review of recent findings and their clinical implications. *Ann Intern Med*. 1977;87:760–768.

27. Saberi M, Sterling FH, Utiger RD. Reduction in extrathyroidal triiodothyronine production by propylthiouracil in man. *J Clin Invest*. 1975;55:218–223.

28. Bianco AC, Kim BW. Deiodinases: implications of the local control of thyroid hormone action. *J Clin Invest*. 2006;116:2571–2579.

29. Chaker L, Ligthart S, Korevaar TI, et al. Thyroid function and risk of type 2 diabetes: a population-based prospective cohort study. *BMC Med*. 2016;14:150.

30. Allaoui G, Rylander C, Averina M, et al. Longitudinal changes in blood biomarkers and their ability to predict type 2 diabetes mellitus—the Tromsø study. *Endocrinol Diabetes Metab*. 2022;5:e00325.

31. Biondi B, Kahaly GJ, Robertson RP. Thyroid dysfunction and diabetes mellitus: two closely associated disorders. *Endocr Rev*. 2019;40:789–824.

32. Gambelunghe G, Forini F, Laureti S, et al. Increased risk for endocrine autoimmunity in Italian type 2 diabetic patients with GAD65 autoantibodies. *Clin Endocrinol (Oxf)*. 2000;52:565–573.

33. Fleiner HF, Bjoro T, Midthjell K, Grill V, Asvold BO. Prevalence of thyroid dysfunction in autoimmune and type 2 diabetes: the population-based HUNT study in Norway. *J Clin Endocrinol Metab*. 2016;101:669–677.

34. Zou J, Li Z, Tian F, et al. Association between normal thyroid hormones and diabetic retinopathy in patients with type 2 diabetes. *Biomed Res Int*. 2020;2020:8161797.

35. Scheef E, Wang S, Sorenson CM, Sheibani N. Isolation and characterization of murine retinal astrocytes. *Mol Vis*. 2005;11:613–624.

36. Dobin A, Davis CA, Schlesinger F, et al. STAR: ultrafast universal RNA-seq aligner. *Bioinformatics*. 2013;29:15–21.

37. Trapnell C, Williams BA, Pertea G, et al. Transcript assembly and quantification by RNA-Seq reveals unannotated transcripts and isoform switching during cell differentiation. *Nat Biotechnol*. 2010;28:511–515.

38. Rathmann D, Rijntjes E, Lietzow J, Köhrle J. Quantitative analysis of thyroid hormone metabolites in cell culture samples using LC-MS/MS. *Eur Thyroid J*. 2015;4:51–58.

39. Bedolla DE, Torre V. A component of retinal light adaptation mediated by the thyroid hormone cascade. *PLoS One*. 2011;6:e26334.

40. Cosentino F, Hishikawa K, Katusic ZS, Lüscher TF. High glucose increases nitric oxide synthase expression and superoxide anion generation in human aortic endothelial cells. *Circulation*. 1997;96:25–28.

41. El-Remessy AB, Abou-Mohamed G, Caldwell RW, Caldwell RB. High glucose-induced tyrosine nitration in endothelial cells: role of eNOS uncoupling and aldose reductase activation. *Invest Ophthalmol Vis Sci*. 2003;44:3135–3143.

42. Huang Q, Sheibani N. High glucose promotes retinal endothelial cell migration through activation of Src, PI3K/Akt1/eNOS, and ERKs. *Am J Physiol Cell Physiol*. 2008;295:C1647–C1657.

43. Miyamoto K, Khosrof S, Bursell SE, et al. Prevention of leukostasis and vascular leakage in streptozotocin-induced diabetic retinopathy via intercellular adhesion molecule-1 inhibition. *Proc Natl Acad Sci USA*. 1999;96:10836–10841.

44. Burlet E, Jain SK. Manganese supplementation reduces high glucose-induced monocyte adhesion to endothelial cells and endothelial dysfunction in Zucker diabetic fatty rats. *J Biol Chem*. 2013;288:6409–6416.

45. Talahalli R, Zarini S, Sheibani N, Murphy RC, Gubitosi-Klug RA. Increased synthesis of leukotrienes in the mouse model of diabetic retinopathy. *Invest Ophthalmol Vis Sci*. 2010;51:1699–1708.

46. Menke A, Casagrande S, Geiss L, Cowie CC. Prevalence of and trends in diabetes among adults in the United States, 1988-2012. *JAMA*. 2015;314:1021–1029.

47. Libman IM, Sun K, Foley TP, Becker DJ. Thyroid autoimmunity in children with features of both type 1 and type 2 diabetes. *Pediatr Diabetes*. 2008;9:266–271.

48. Fatourechi A, Ardakani HM, Sayarifard F, Sheikh M. Hypothyroidism among pediatric patients with type 1 diabetes mellitus, from patients' characteristics to disease severity. *Clin Pediatr Endocrinol*. 2017;26:73–80.

49. Aoki T, Tsunekawa K, Araki O, et al. Type 2 iodothyronine deiodinase activity is required for rapid stimulation of PI3K by thyroxine in human umbilical vein endothelial cells. *Endocrinology*. 2015;156:4312–4324.

50. Ettleson MD, Bianco AC. Individualized therapy for hypothyroidism: is T4 enough for everyone? *J Clin Endocrinol Metab*. 2020;105:e3090–3104.

51. Castagna MG, Dentice M, Cantara S, et al. DIO2 Thr92Ala reduces deiodinase-2 activity and serum-T3 levels in thyroid-deficient patients. *J Clin Endocrinol Metab*. 2017;102:1623–1630.